AGU PUBLICATIONS

JGR

Journal of Geophysical Research: Oceans

RESEARCH ARTICLE

10.1002/2016JC012465

Key Points:
- DMS heterogeneity and turnover rate increased from oceanic waters shoreward
- DMS concentrations were correlated with biological oxygen accumulation and upwelling intensity in coastal waters
- DMS turnover rates are significantly correlated with observed DMS concentrations

Supporting Information:
- Supporting Information S1
- Data Set S1

Correspondence to:
E. Asher,
ecasher@ucdavis.edu

Citation:
Asher, E., J. W. Dacey, D. Ianson, A. Peña, and P. D. Tortell (2017), Concentrations and cycling of DMS, DMSP, and DMSO in coastal and offshore waters of the Subarctic Pacific during summer, 2010-2011, *J. Geophys. Res. Oceans*, *122*, 3269–3286, doi:10.1002/2016JC012465.

Received 12 OCT 2016
Accepted 22 FEB 2017
Accepted article online 28 FEB 2017
Published online 24 APR 2017

Concentrations and cycling of DMS, DMSP, and DMSO in coastal and offshore waters of the Subarctic Pacific during summer, 2010-2011

Elizabeth Asher[1], John W. Dacey[2], Debby Ianson[1,3], Angelica Peña[3], and Philippe D. Tortell[1,4,5]

[1]Department of Earth, Ocean and Atmospheric Sciences, University of British Columbia, Vancouver, British Columbia, Canada, [2]Biology Department, Woods Hole Oceanographic Institution, Woods Hole, Massachusetts, USA, [3]Institute of Ocean Sciences, Fisheries and Oceans Canada, Sidney, British Columbia, Canada, [4]Botany Department, University of British Columbia, Vancouver, British Columbia, Canada, [5]Peter Wall Institute for Advanced Studies, University of British Columbia, Vancouver, British Columbia, Canada

Abstract Concentrations of dimethylsulfide (DMS), measured in the Subarctic Pacific during summer 2010 and 2011, ranged from ~1 to 40 nM, while dissolved dimethylsulfoxide (DMSO) concentrations (range 13-23 nM) exceeded those of dissolved dimethyl sulfoniopropionate (DMSP) (range 1.3–8.8 nM). Particulate DMSP dominated the reduced sulfur pool, reaching maximum concentrations of 100 nM. Coastal and off shore waters exhibited similar overall DMS concentration ranges, but sea-air DMS fluxes were lower in the oceanic waters due to lower wind speeds. Surface DMS concentrations showed statistically significant correlations with various hydrographic variables including the upwelling intensity ($r^2 = 0.52$, $p < 0.001$) and the Chlorophyll *a*/mixed layer depth ratio ($r^2 = 0.52$, $p < 0.001$), but these relationships provided little predictive power at small scales. Stable isotope tracer experiments indicated that the DMSP cleavage pathway always exceeded the DMSO reduction pathway as a DMS source, leading to at least 85% more DMS production in each experiment. Gross DMS production rates were positively correlated with the upwelling intensity, while net rates of DMS production were significantly correlated to surface water DMS concentrations. This latter result suggests that our measurements captured dominant processes driving surface DMS accumulation across a coastal-oceanic gradient.

Plain Language Summary The trace gas dimethyl sulfide is a precursor for natural, sulfur-based aerosols that influence climate, an important compound in marine microbial communities, and an olfactory foraging cue for seabirds. This article discusses data from two surveys of dimethyl sulfide in 2010 and 2011 in the Subarctic Northeast Pacific ocean. The surveys consisted of extensive concentration measurements across this region and in specific locations, novel rate measurements of the biological and chemical production and removal of this gas. We found that dimethyl sulfide concentrations may be predicted from the measured rates of its production and consumption. In coastal waters, dimethyl sulfide concentrations appear related to the supersaturation of biological oxygen in surface waters.

1. Introduction

Dimethylsulfide (DMS) is a biogenic sulfur compound derived from the algal metabolite dimethyl sulfoniopropionate (DMSP) in marine surface waters. *Lovelock et al.* [1972] revealed an important role for dimethyl sulfide (DMS) in the global sulfur budget, stimulating decades of subsequent research into the oceanic cycling of this compound. There has been significant discussion of the potential role of DMS in climate regulation, as a precursor to sulfate aerosols that backscatter incoming solar radiation and promote cloud formation [*Charlson et al.*, 1987; *Quinn and Bates*, 2011]. Moreover, this compound (along with DMSP, and dimethylsulfoxide, DMSO) is key to the metabolism of many marine microbes, as a source of reduced carbon and sulfur [*Kiene et al.*, 2000; *Howard et al.*, 2006; *Reisch et al.*, 2011]. DMS and DMSP may also act as chemotactic attraction compounds for predators [*Seymour et al.*, 2010; *Nevitt*, 2008], thus providing a biogeochemical link across different trophic levels of the marine ecosystem. With some recent exceptions [e.g., *Royer et al.*, 2016], most models have employed crude and implicit parameterizations of both bacterial DMS

production and rates of DMS production and biological consumption rates that reflect changes in environmental variables [*Le Clainche et al*., 2010].

Biogeochemical processes and ecological dynamics influence surface ocean DMS concentrations over a range of spatial and temporal scales. Global-scale oceanographic databases have been used to develop empirical algorithms correlating DMS concentrations with a variety of biophysical variables, such as the ratio of chlorophyll to mixed layer depths (MLD) [*Simo and Dachs*, 2002; *Belviso et al*., 2004; *Nemcek et al*., 2008], ultraviolet radiation (UV) [*Sunda et al*., 2002], the solar radiation dose [*Vallina and Simo*, 2007], and phytoplankton taxonomy [*Masotti et al*., 2010]. Attempts have been made to use these parameterizations to predict DMS responses to climate perturbations in global climate models [e.g., *Halloran et al*., 2010].

On a regional scale, time-series observations have increased our understanding of the temporal dynamics of DMS/P/O with respect to environmental forcing. The most comprehensive DMS/P/O time-series observations have been conducted in the Sargasso Sea as part of the Bermuda Atlantic Time Series (BATS) program [*Dacey et al*., 1998; *Levine et al*., 2012], which has documented moderate seasonality and interannual variability in surface DMS concentrations (range 1-7 nM) in subtropical waters of the N. Atlantic. These dynamics appear to reflect changes in the net balance of bacterial and algal DMS consumption or production, and in the activity of DMSP lyase, an enzyme that produces DMS during the cleavage of DMSP. Unfortunately, insight gained from DMS time-series work at BATS may not translate directly to other oceanic regions, which experience significantly different environmental forcing regimes. In particular, subpolar and polar marine waters are known to be oceanic DMS "hotspots," where extremely high DMS concentrations ($>$20 nM) are observed during the summer. These regions with persistently high DMS concentrations include a number of Antarctic polynyas [*DiTullio and Smith*, 1995; *Tortell et al*., 2011; *Tortell et al*., 2012a] and the open ocean waters of the Subarctic Pacific [*Steiner et al*., 2012].

Over the past decade, the Line P time-series program has documented seasonal and interannual variability in surface water DMS concentrations in the Northeast Subarctic Pacific. Surface water DMS concentrations along the Line P transect are characterized by significant spatial variability (over a range of length scales) and large potential interannual variability [*Asher et al*., 2011a; *Steiner et al*., 2012]. The region comprises two distinct ecological provinces; a high productivity coastal regime, and an iron (Fe)-limited, high nutrient and low chlorophyll (HNLC) offshore regime [*Harrison et al*., 1999; *Martin and Fitzwater*, 1988]. Maximum DMS concentrations in excess of 20 nM ($\sim$10-fold higher than the global average) have been observed in HNLC open ocean waters along Line P during the late summer and early fall. Field observations and modeling results have suggested that the phytoplankton speciation and iron nutrient limitation of these phytoplanktons are dominant factors driving perennial summer-time DMS accumulation in these offshore HNLC waters [*Levasseur et al*., 2006; *Lizotte et al*., 2009; N. Steiner, personal communication, 2012]. Iron limitation has been shown to increase cellular production of DMS and DMSP, potentially as a physiological response to oxidative stress. In conjunction with rapid biological cycling, physical processes such as entrainment, sea-air exchange and photo-oxidation of DMS to DMSO (Figure 1) have also been shown to drive temporal changes in DMS at Ocean Station Papa [e.g., *Le Clainche et al*., 2006], the western most station along the Line P transect.

Continental shelf waters along the British Columbia (BC) coast have also attracted recent attention as a seasonally strong but variable source of DMS [*Sharma et al*., 1999; *Nemcek et al*., 2008; *Tortell et al*., 2012b]. These productive coastal waters receive significant iron inputs from shelf sediments, and are characterized by complex shelf bathymetry, summertime wind-driven upwelling (Figure 1), and the presence of several strong near shore current systems, namely the southbound California Current and northbound Vancouver Island Coastal Current (VICC) [*Cullen et al*., 2009; *Freeland et al*., 1984]. In this coastal region, physical dynamics lead to strong spatial and temporal variability in macronutrient supply, which drives significant variability in phytoplankton biomass, speciation, and productivity. This variability may, in turn, lead to strong temporal and spatial gradients in the surface water concentrations of DMS and other biogenic gases [*Nemcek et al*., 2008, *Evans et al*., 2012; *Tortell et al*., 2012b]. To date, however, DMS dynamics in the continental shelf waters of the Subarctic Northeast (NE) Pacific remain less well studied than those in the offshore region.

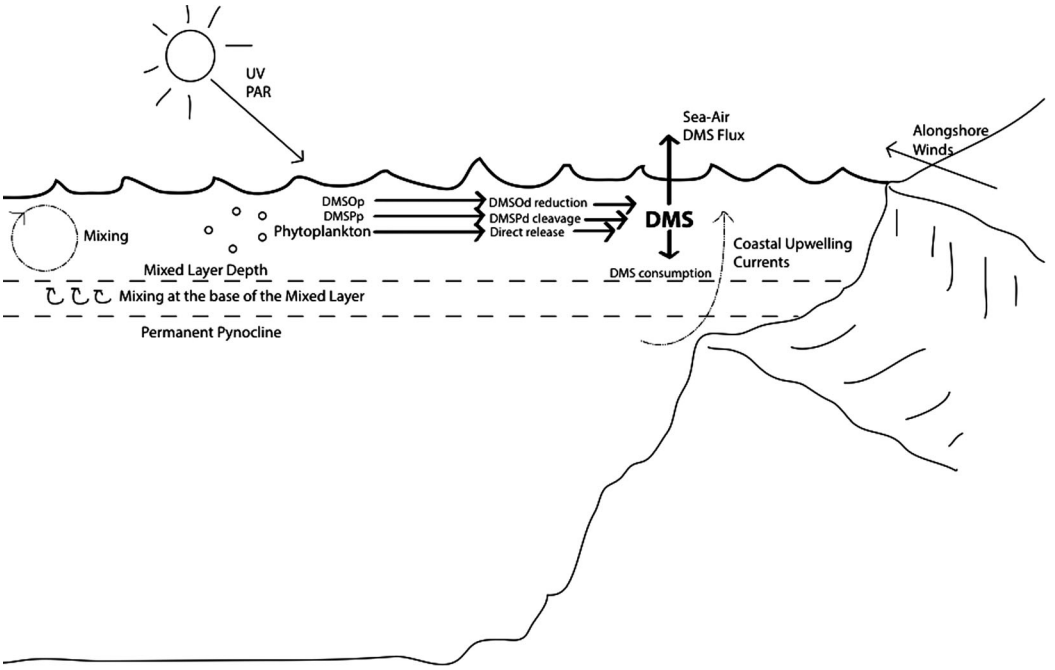

Figure 1. A schematic of surface ocean DMS production and removal pathways as they relate to physical and meteorological forcing in the Subarctic NE Pacific.

Despite recent progress toward documenting the spatial and temporal variability of DMS concentrations in the Subarctic NE Pacific [e.g., *Wong et al*., 2005; *Asher et al*., 2011a; *Tortell et al*., 2012b], fundamental gaps remain in our understanding of the underlying processes of DMS production and removal. In general, dissolved DMSP ($DMSP_d$) cleavage is considered to be the main pathway for oceanic DMS production, and this process can be mediated either by phytoplankton that possess intracellular DMSP lyase, or by bacteria acting on the dissolved DMSP pool in seawater. As a result, the relative importance of phytoplankton versus bacteria to DMS production remains a topic of particular interest. Abiotic photooxidation of DMS to DMSO, and biological (largely bacterial) DMS consumption can both contribute significantly to DMS removal (Figure 1), with their relative importance depending on solar (UV) intensity, mixed layer depth and the activity, taxonomic composition and sulfur requirements of bacterial assemblages [*Le Clainche et al*., 2006]. To date, two studies have employed radio-isotope ^{35}S labeling methods to examine DMS cycling in the Subarctic Pacific [*Merzouk et al*., 2006, *Royer et al*., 2010]. While this work has provided important information on DMS production/consumption processes, the key rates of the DMS cycle (DMS production from $DMSP_d$ cleavage and DMS consumption; Figure 1) have not been measured simultaneously in Subarctic Pacific waters. Moreover, no studies to date have examined the potential contribution of DMSO reduction to DMS cycling in this region (Figure 1). Recent work in Antarctic polynyas [*Asher et al*., 2011b], suggests that this process may be important in at least some marine environments.

To examine the distribution and cycling of DMS, DMSP, and DMSO in the Subarctic Pacific Ocean, we conducted high spatial resolution surface DMS surveys using membrane inlet mass spectrometry (MIMS), and quantified DMS turnover across coastal, transitional, and open ocean waters. We also employed a relatively new tracer-based method [*Asher et al*., 2011b] to simultaneously quantify key processes in the DMS cycle, namely gross DMS removal, DMSP cleavage, and DMSO reduction [*Asher et al*., 2011b]. Our results demonstrate consistent differences in DMS concentrations and dynamics across a coastal-oceanic gradient. Moreover, we show that correlations between DMS concentrations and various oceanographic variables (e.g., upwelling intensity and biological oxygen accumulation) can be observed at various spatial scales, but have little predictive power across multiple scales. We also show that measured DMS turnover rates are significantly correlated with observed DMS concentrations, suggesting that our rate measurements capture the dominant processes leading in DMS accumulation in surface waters.

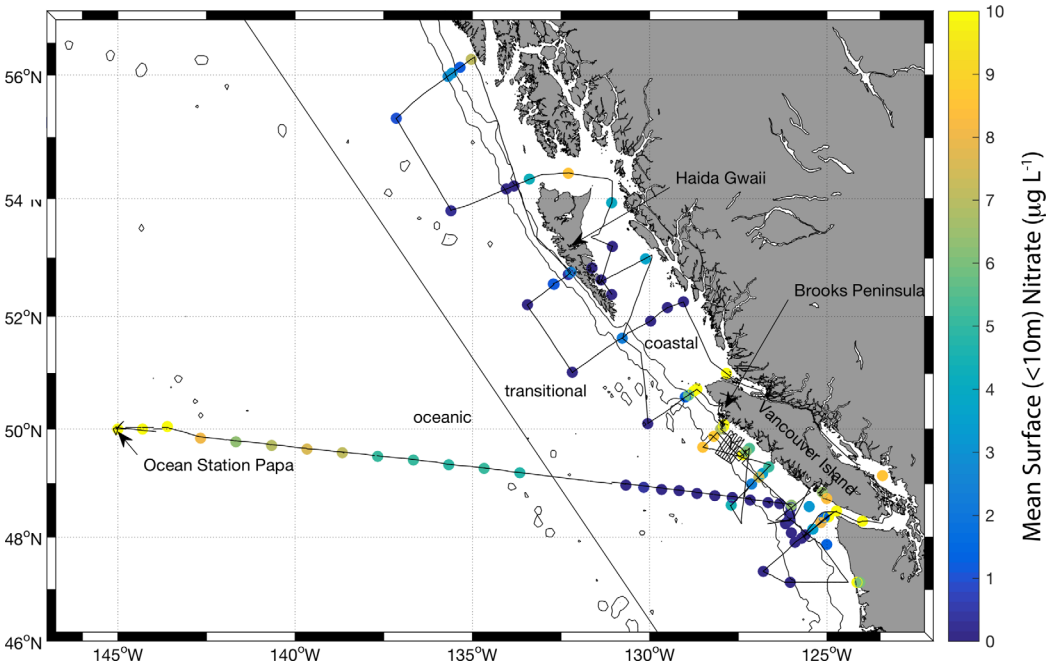

Figure 2. Ship cruise tracks and surface water (<10 m) nitrate concentrations in coastal and open ocean waters of the Subarctic NE Pacific in late summer of 2010 and 2011. The 2000 m isobath, which is taken as the boundary between coastal and transitional waters, and the 500 m isobath are also shown for reference. A nitrate threshold of >1μM is used as the boundary between transitional and open ocean waters, and denoted by the straight diagonal line on the figure. Text labels indicate geographic and oceanographic regions and locations of interest: Haida Gwaii, Vancouver Island, Brooks Peninsula, Ocean Station Papa, oceanic, transitional, and coastal waters.

2. Methods

2.1. Field Sampling

We conducted two research cruises on board the *CCGS John P. Tully*, surveying coastal and open ocean regions of the Subarctic NE Pacific (Figure 2). Coastal waters of BC were surveyed between 20 July and 15 August 2010 on the West Coast Acidification Cruise (WCAC; cruise IOS-2010-36). The cruise track (Figure 2) covered the outer coast of Vancouver Island, Haida Gwaii and much of the central BC coast. Stations were sampled along the continental shelf, and on a number of cross-shelf transects. During this cruise, we also had the opportunity to sample a detailed grid near the Brooks Peninsula (∼127.9 W, 50.1°N), during a two day search and rescue (SAR) mission. During the summer of 2011, we sampled along the Line P time-series transect (from Vancouver Island to Ocean Station Papa, 145°W, 45°N) from 16 August to 1 September 2011 (cruise IOS-2011-27). The westward and returning eastward ship tracks for this cruise were conducted along the same survey line, providing us with an opportunity to sample similar waters masses on outward and return legs. The time interval between outbound and return occupations of areas ranges from less than two days in the most offshore waters to approximately two weeks for the near-shore regions.

2.2. Surface Water Gas Measurements

Surface water DMS was measured using membrane inlet mass spectrometry (MIMS) [*Tortell*, 2005], following the procedures outlined in *Tortell et al.* [2011]. Briefly, surface seawater obtained from the ship's intake (∼5 m depth) was pumped through a sampling cuvette at 500 ml min^{-1}, allowing gases to permeate across a ∼0.25 mm thick dimethylsilicone membrane into a Hiden Analytical quadropole mass spectrometer. Sample water temperature was maintained at 15°C, using ∼6 m of stainless steel tubing immersed in a water bath immediately upstream of the sampling cuvette. Measurements were made every ∼30 s, which is equivalent to ∼200 m spatial resolution at cruising speeds of 5-10 kn. DMS partial pressures were calibrated from raw ion current intensities every ∼1 to 2 days using known DMS standards made from liquid DMS diluted with 1 L of deep (> 200 m) seawater. MIMS was also used to measure net biological oxygen production in surface waters based on the ratio of measured O_2/Ar ratios relative to atmospheric equilibrium values (i.e., ΔO_2/Ar).

2.3. DMS/P/O Concentration Measurements

For the analysis of total (i.e., unfiltered seawater) DMS_t, $DMSP_t$, and $DMSO_t$ concentrations, we collected 1 L samples in UV transparent (UVT) bags from Niskin bottles and dispensed 10 mL duplicate subsamples into 20 mL acid-cleaned, transparent serum vials with Teflon faced caps (Wheaton PN 224100). DMS was sparged out of solution under N_2 flow and analyzed using a purge and trap capillary inlet mass spectrometer (PT-CIMS), as described by *Asher et al.* [2011b]. Additional details of this method are provided in supporting information. After DMS sparging and analysis, samples were treated with either 2 mL of 10 N NaOH (for DMSP samples) or 2 mL of $TiCL_3$ (for DMSO samples), capped with teflon faced caps and allowed to sit for 12-24 h. Prior to analysis, duplicate subsamples for dissolved DMSP and DMSO were gently filtered through 0.2 μm acrodisc syringe filters according to *Kiene and Slezak* [2006]. All discrete concentration measurements, including those for DMS production and removal rate measurements were conducted using PT-CIMS to follow the concentrations of isotopically-labeled S compounds (see supporting information for details). Concentrations were calculated based on the linear relationship between peak area and known concentrations of standards made from diluted stocks of liquid DMS, DMSP and DMSO approximately every three days ($r^2 \geq 0.98$).

2.4. Rate Experiments

Rate experiments were conducted using either a competitive inhibition (CI) approach, or with isotope tracer additions, as previously described by *Asher et al.* [2011b]. While both approaches offer valuable information on the balance of gross DMS production and gross DMS removal, tracer experiments have the added advantage of simultaneously quantifying the relative importance of DMS production from different reduced sulfur pools (i.e., DMSP vs. DMSO).

For all rate experiments, seawater samples were collected from 10 m depth with Niskin bottles and homogenized inside a 20 L carboy by inverting the container ~10 times. Three liter volumes were dispensed into triplicate UV transparent FEP plastic bags (Welch Fluorocarbon – P00020-1) using a graduated cylinder (we note that our initial (T_0) concentration measurements of natural DMS may be lower due to gas exchange that occurred during the sample handling). Bags were incubated in deck-board seawater tanks, maintained at situ surface temperature using flowing seawater. Ambient light levels were reduced to ~30% of surface values using two layers of neutral density screening. Bags were gently inverted 10-15 times to mix the tracer and competitive inhibitor additions before initial T_0 subsamples were removed within 20 min. Subsamples were removed from the bags, using a 60 mL syringe via a luer lock port, and loaded onto a rack for automated sampling and PT-CIMS analysis every 1.5-2 h.

Several postprocessing steps were required to obtain rate constants from the raw data from tracer and competitive inhibitor experiments. Rate constants for gross DMS production in CI experiments were derived from the slope of the natural logarithm of unlabeled DMS/P concentrations over time (equations (1) and (2)). First, however, unlabeled (i.e., m/z 62) DMS concentrations in DMS CI experiments were corrected for ~1% ion source mass fragmentation from the m68 DMS (http://webbook.nist.gov/), which was added as a competitive inhibitor at > 20 times the concentration of background DMS.

$$\mathrm{natural\ DMS} = m62\ DMS - 0.01\ X\ m68\ DMS \tag{1}$$

$$\ln \frac{[\mathrm{natural\ DMS}]}{[\mathrm{natural\ DMS}]_0} = -k_{DMS_production}\ t \tag{2}$$

For isotope tracer experiments, we amended four replicate bags with near tracer level (i.e. < ~20% of ambient) additions of D-3 deuterated DMS, D-6 deuterated DMSP, and ^{13}C labeled DMSO [see *Asher et al.*, 2011b] to achieve final concentrations of 1, 0.7, and 0.5 nM, respectively. DMS removal was calculated as a pseudo first-order reaction:

$$\ln \frac{[D-3\ DMS]}{[D-3\ DMS]_0} = -k_{DMS,emoval}\ t \tag{3}$$

where k_{dms_cons} is the observed rate constant, t is time, and [D-3 DMS] is the concentration of the added tracer (equation (1)). The m/z 64 signal, indicative of C-13_2 labeled DMS derived from $DMSO_d$, was corrected for the background pool of S_{34}-containing DMS and ion source fragmentation;

$$[C13_2{-}DMS] = [DMS_{64}] - 0.3\ [DMS_{65}] - 0.043\ [DMS_{62}] \quad (4)$$

To calculate a gross $DMSO_d$ reduction rate, we corrected the measured concentration of C-13_2 labeled DMS for gross DMS removal, as measured using D-3 DMS tracer;

$$[C13_2DMS]_{corrected} = [C13_2DMS] + \frac{[C13_2DMS]_0}{e^{-k_{DMSr\,emoval}t}} \quad (5)$$

Similarly, we corrected the D-6 DMS concentrations for gross DMS removal (equation (1)) to calculate a gross $DMSP_d$ cleavage rate as:

$$[D{-}6\ DMS]_{corrected} = [D{-}6\ DMS] + \frac{[D{-}6\ DMS]_0}{e^{-k_{DMSr\,emoval}t}} \quad (6)$$

Gross $DMSO_d$ reduction and $DMSP_d$ cleavage were computed in a manner similar to gross DMS removal (though opposite in sign). We used the slope of the natural logarithm of corrected C-13_2 and D-6 labeled DMS concentrations over time to calculate the respective rate constants.

$$\ln \frac{[C13_2{-}DMS]_{corrected}}{[C13_2{-}DMS]_{0\ corrected}} = K_{DMSO,eduction}t \quad (7)$$

$$\ln \frac{[D{-}6\ DMS]_{corrected}}{[D{-}6\ DMS_0]} = K_{cleavage}t \quad (8)$$

If the initial T_0 C-13_2 or D-6 DMS concentrations were below the 0.1 nM detection limit, we assumed an initial concentration of 0.1 nM. For all rate constant calculations, we report uncertainty as one standard error from the mean slope in these experiments. To determine natural removal and production terms (nM d^{-1}), rate constants measured in the experimental bags were multiplied by in situ concentrations of DMS, DMSP, and DMSO. Standard error propagation was used to extend the uncertainty of rate constant measurements and in situ DMS/P/O concentrations to natural production and removal terms (nM d^{-1}).

2.5. Ancillary Measurements

We used a series of additional measurements to provide a biogeochemical and biophysical context for our DMS data. All ancillary data described below for the Line P cruise are publicly available (http://www.pac.dfo-mpo.gc.ca/science/oceans/data-donnees/line-p/2011-27/index-eng.htm). The mixed layer depth (MLD) was calculated using a 0.125 kg/m^{-3} density difference ($\Delta\sigma_\tau$) criterion [*Levitus*, 1982] from the density profile (downcast data only) at each station. The calculation did not appear particularly sensitive to various density criteria, although this simplistic 0.125 kg/m^{-3} $\Delta\sigma_t$ criterion may reflect the residual mixed layer (from recent past days) more so than the actively mixing layer [*Brainerd and Gregg*, 1995]. Density profiles were calculated using conservative temperature and absolute salinity. These variables were derived from CTD-measurements of temperature and practical salinity using the Gibbs Oceanographic Toolbox for MATLAB (http://www.teos-10.org/pubs/gsw/html/gsw_contents.html). Chlorophyll *a* (Chl*a*) and nitrate concentrations were determined by fluorometeric analysis [*Holm-Hansen et al*., 1965] and auto-analyzer methods [*Barwell-Clarke and Brabant*, 1996], respectively. The contribution of various phytoplankton taxa to chl*a* concentrations was determined from HPLC measurements of accessory photosynthetic pigment concentrations [*Mackey et al*., 1996; *Zapata et al*., 2000], followed by CHEMTAX analysis.

2.6. Sea-Air Flux

DMS sea-air fluxes along the cruise tracks were calculated using aqueous MIMS DMS concentrations and piston velocities (k_w), derived from wind speeds, surface temperature and salinity (equation (9)):

$$DMS\ Flux = k_w\ [DMS]_{aq} \quad (9)$$

The Schmidt number used for these calculations was derived using the equation of *Saltzman et al*. [1993]. Ship's wind speed data were not available due to a malfunction of the anemometer. Thus, daily 10 m wind speeds for the 2010 WCAC were obtained from environment Canada buoys located between 48°N and 55°N and 124°W and 140°W (http://www.ndbc.noaa.gov/index.shtml). For the 2011 Line P cruise, NCEP Reanalysis II 10 m daily winds from 2011 were used (http://www.esrl.noaa.gov/psd/data/gridded/data.ncep.reanalysis2.gaussian.html). DMS fluxes in 2010 and 2011 were calculated using the wind-speed

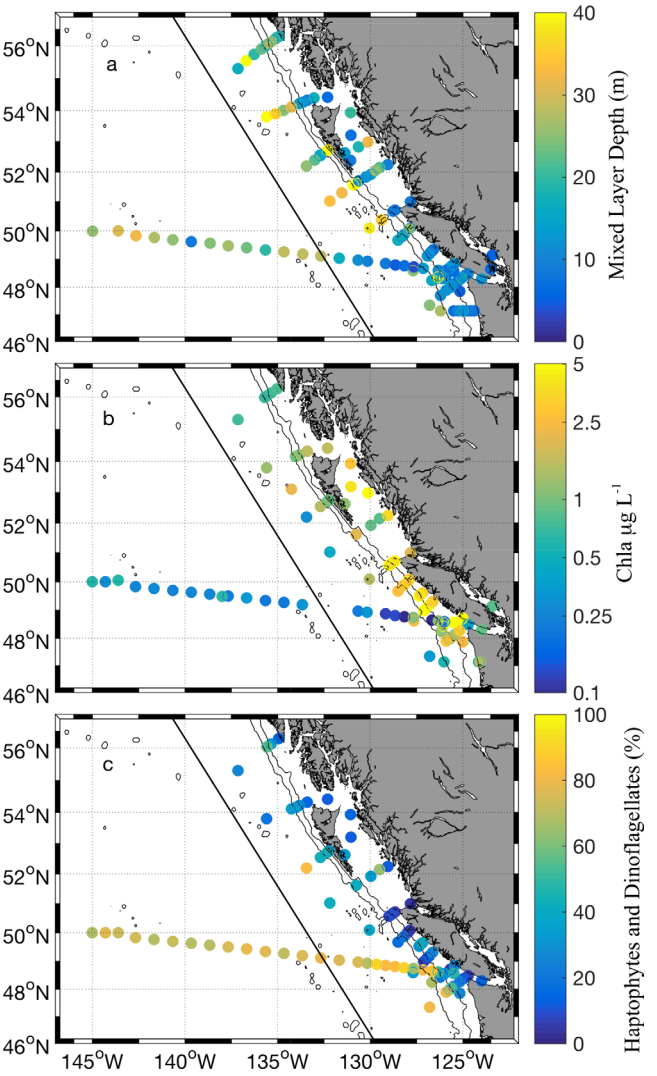

Figure 3. (a) CTD-derived mixed layer depth, (b) chl*a* measured from ~5 m rosette bottle casts, and (c) the relative abundance of Haptophyte and Dinoflagellate chl*a* at ~5 m in summer of 2010 and 2011. The color scale for Chlorophyll is logarithmic. For reference, the transitional-open ocean boundary, as well as the 500 m and 2000 m isobaths, (the latter of which serves as the coastal-transitional boundary), are marked.

parameterization of *Ho et al.* [2006]. DMS removal rates (nM d^{-1}) in the mixed layer due to air-sea flux were computed by dividing flux (μmol m^{-2} d^{-1}) by the mixed layer depth (m). For comparison, these rates were divided by the in situ concentration of DMS (nM) to yield rate constants (d^{-1}) of DMS removal in surface waters due to air-sea flux, and a corresponding physical residence time τ_{Dms} (days).

3. Results

3.1. Hydrography and Plankton Biomass Distributions in Coastal and Open Ocean Waters

Our sampling region encompassed several distinct oceanographic regimes, from high productivity coastal upwelling waters to iron-limited HNLC regions. A transitional region, subject to coastal and offshore influences, separated these waters. For the purpose of this study, we define the boundary between coastal waters and transitional waters as the 2000 m isobath, according to *Asher et al.* [2011a], and the boundary between transitional waters and open-ocean HNLC waters as a threshold value in summer time surface nitrate concentrations greater than 1 µM. In the offshore region, the presence of excess nutrients in late summer surface waters can be used as a proxy for iron limitation [*Martin and Fitzwater*, 1988; *Royer et al.*, 2010]. Based on surface water concentrations of nitrate, it appears that Fe limitation was apparent west of station P15, (i.e., ~133°W) during our 2011 cruise.

We observed differences in hydrographic and biological properties across the oceanographic regimes in 2010 and 2011. Coastal BC waters, shoreward of the 2000 m isobaths, exhibited shallow mixed layer depths on average (Figure 3a and Table 1). We found mixed layer depths of less than 10 m in regions influenced by a near surface halocline and mixed layer depths of more than 20 m in upwelling areas. By comparison, oceanic and transitional regimes contained higher salinity in surface waters and deeper mixed layer depths on average ($\geq$ 20 m) (Figure 3a and Table 1). Phytoplankton biomass was highest in coastal waters with maximum values $\geq$ 5 μg chl*a* L^{-1} (Figure 3b). In the offshore HNLC waters, chl*a* concentrations were generally low (<0.5 μg L^{-1}), although a small apparent phytoplankton bloom was observed in the vicinity of Ocean Station P, where chl*a* concentrations up to 0.9 μg L^{-1} were observed. The apparent phytoplankton bloom was also captured in eight day composite Aqua MODIS satellite chl*a* imagery. Phytoplankton biomass in the transitional waters was intermediate between that observed in coastal and oceanic waters (Figure 3b and Table 1).

The proportion of Haptophyte and Dinoflagellate phytoplankton (%) (Figure 3c and Table 1) revealed an oceanic-coastal gradient with the highest proportion of these two groups observed in the open ocean. We

Table 1. Oceanographic Properties, DMS Concentrations, and Sea-Air Fluxes Across Contrasting Oceanographic Regimes[a]

Properties	Region	Mean	SD	SE	Range	N
MLD (m)	Oceanic	24	7.4	2.3	9–33	10
	Transitional	26	19	3.1	3.8-100	39
	Coastal	15	13	1.8	5.1-81	82
Salinity (psu; 5 m)	Oceanic	32.34	0.24	4.4E−3	31.69-32.56	∼2800
	Transitional	32.21	0.20	5.5E−3	31.46-32.57	∼1400
	Coastal	31.80	0.57	7.7E−3	27.58-33.21	∼5400
Chl *a* (μg L^{-1}; 10 m)	Oceanic	0.54	0.44	0.13	0.24-1.8	12
	Transitional	0.91	0.87	0.42	0.090-9.4	28
	Coastal	3.4	3.5	0.51	0.095-14	48
Din+Hap Chl*a* (5 m)	Oceanic	0.21	5.3E−2	1.7E−2	0.12-0.32	10
	Transitional	0.38	0.29	5.6E−2	0.051-1.2	28
	Coastal	0.72	0.85	7.5E−3	0.18-4.3	50
DMS (nM; 5 m)	Oceanic	8.4	5.3	9.3E−2	0.46-33	∼3300
	Transitional	5.9	5.4	0.14	0.19-41	∼1500
	Coastal	9.7	7.2	8.0E−2	0.19-42	∼8000
Sea-Air Flux (μmol m^{-2} d^{-1})	Oceanic	14	12	0.21	<1–74	∼3300
	Transitional	11	11	0.28	<1–100	∼1500
	Coastal	7.2	6.7	8.1E−2	<1-100	∼8000

[a]Data from the WCAC in 2010 and Line P in 2011 were pooled to illustrate the spatial variability by oceanographic region across the Subarctic Pacific Ocean in summer. Samples sizes for high resolution underway measurements are based on an estimate of the number of statistically independent data using the mean squared error technique [see *Asher et al*., 2011a].

also observed a difference in the proportion of these groups between the WCAC in 2010 (∼30%) and the Line P in 2011 (∼80%). The remainder of the phytoplankton community was primarily composed of diatoms on the WCAC (∼60%) and an equal mix of diatoms and pelagophytes on the Line P (∼20%; see supporting information for details).

3.2. High Frequency Measurements of DMS Concentrations

Our data revealed a wide range of surface water DMS concentrations (range 0.19-42 nM), with significant fine-scale variability (Figure 4a). On average, higher DMS concentrations occurred in coastal and open ocean waters with moderate DMS concentrations and lower variability in transitional waters (Table 1). Spatial features of note include the accumulation of high DMS concentrations in the offshore waters near station P, high DMS around the Vancouver Island shelf break, and a distinct patch of moderate (∼10 nM) DMS concentrations in the transitional waters. We used a mean square error technique to estimate the number of statically independent data points [*Asher et al*., 2011a] in each oceanographic region. From this, we estimate that our MIMS data comprises more than ∼1000 independent measurements in each region, yielding small standard errors of the mean DMS concentrations. As a result, differences between the mean DMS concentrations in the three oceanographic domains are statistically significant, despite large variability within each domain.

At several locations across our survey region, DMS hotspots also often overlapped with regions of high ΔO_2/Ar and strong gradients in surface salinity, particularly in transitional waters (Figures 4b and 4c). Increased DMS concentrations (∼10 nM) were observed in the vicinity of a salinity frontal zone across the 2000 m isobath at 54.0°N, in the transitions waters at ∼130.7°W, and in regions of high salinity recently upwelled water North of the Brooks Peninsula.

3.3. High-Resolution Survey of DMS Across the Shelf-Break

We conducted a detailed survey of DMS concentrations in coastal BC surface waters, as part of a search and rescue exercise along the Brooks Peninsula (Figure 5). Over the course of approximately three days, we measured strong concentration gradients in DMS (i.e., ∼0.5 to ∼40 nM) (Figure 5a), and significant variability in biological oxygen accumulation (ΔO_2/Ar −20 to 20%; Figure 5b), sea surface salinity (∼31.7 to 32.7 PSU; Figure 5c), and temperature (∼9 to 15°C; data not shown). The highest DMS concentrations (>30 nM) were observed in upwelling regions with high salinity, low temperature waters north of the peninsula (Figure 5). Lower DMS concentrations (∼10 nM) were measured southwest of the peninsula, and moderately elevated DMS concentrations (15-20 nM) were observed southeast of the peninsula near steep gradients in surface salinity (31.8 to >32.4 PSU; Figure 5c).

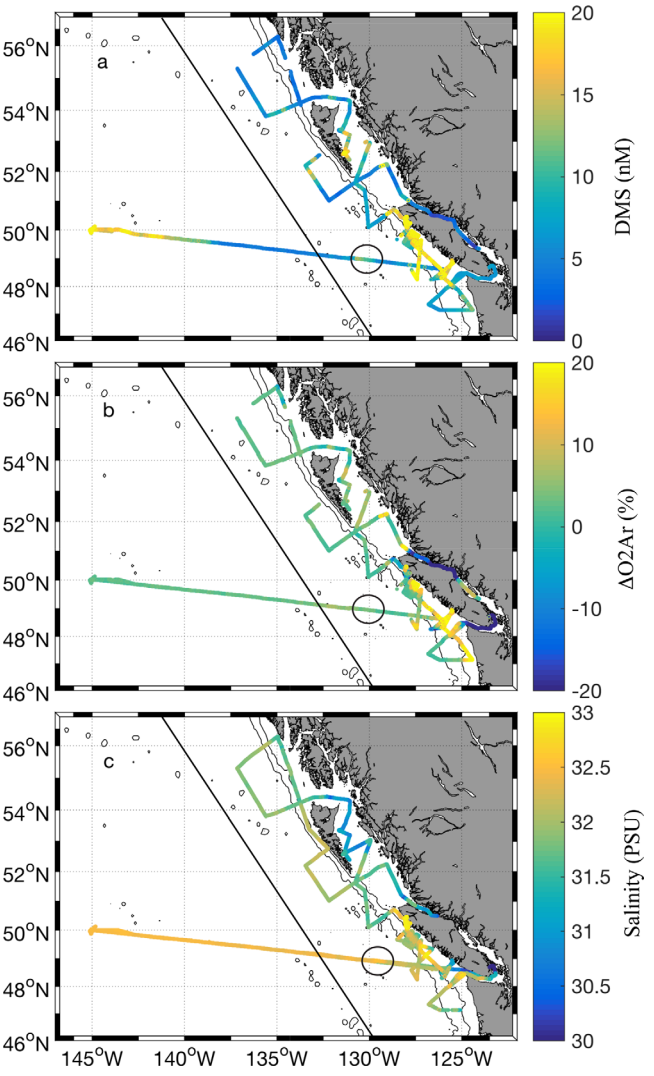

Figure 4. Spatial distribution of (a) DMS concentrations, (b) $\Delta O_2/Ar$, and (c) salinity in coastal and offshore waters of the NE Subarctic Pacific during late summer 2010 and 2011. For reference, the DMS hotspot at ~130.7W and the coastal-transitional and transitional-open ocean boundaries is marked by a circle. Although the maximum DMS concentrations and $\Delta O_2/Ar$ saturation values exceed the upper bounds of the scales used below, (a) the 0-20 nM scale and (b) −20 to 20% scale are used to highlight the heterogeneity in DMS and $\Delta O_2/Ar$ across our survey region in 2010 and 2011. For reference, the transitional-open ocean boundary, as well as the 500 m and 2000 m isobaths, (the latter of which serves as the coastal-transitional boundary), are marked.

DMS concentrations appeared to be highly dynamic over the short time of our survey, with repeated measurements showing significant differences in DMS levels in crossover transects. For instance, between 3 August and 8 August, 49° 36N and 127° 30'W, we observed striking differences in DMS concentrations and sea surface salinity patterns (Figure 5d). These rapid temporal dynamics highlight the challenges involved in sampling across space and time given the rapid biological (and chemical) cycling of DMS in surface waters. We note that this temporal analysis is significantly complicated by complex physical dynamics and potential for water mass advection. In the absence of a truly Lagrangian approach, the differences we observed in surface water properties likely reflect the combination of true temporal dynamics and water mass advection.

Within the SAR study area of the WCAC cruise, we investigated the relationship between DMS concentrations and other major gases and hydrographic parameters (e.g., temperature, salinity, $\Delta O_2/Ar$). As shown in Figure 6, we were able to derive a statistically significant multiple linear regression model predicting DMS concentrations from $\Delta O_2/Ar$ and sea surface salinity (without any interaction terms). This statistical model ($DMS = -462 + 0.38\ \Delta O_2/Ar + 14.8\ Sal$; $F\text{-stat} = 7607$, $p < 0.01$) was able to explain the observed variability in DMS concentrations. In this coastal region, high DMS was associated with saline, recently upwelled waters, and high biological activity near the shelf break. The relatively large residual variation in DMS (even within a small sampling region and time window) reveals the complex dynamics that drive DMS cycling in coastal waters.

3.4. Empirical Algorithms and DMS Distributions

As in previous studies [*Asher et al.*, 2011a; *Tortell et al.*, 2012b], we found few statistically significant correlations between surface water DMS concentrations and other ancillary oceanographic variables. DMS concentrations in coastal and transitional waters south of 51°N were best explained ($r^2 = 0.52$, $F = 12.82$, $p < 0.001$) by a multiple regression including $\Delta O_2/Ar$, sea surface temperature, and upwelling intensity derived from the Bakun upwelling index. For this latter variable, we found the highest correlation using upwelling intensity at 36°N with a four day time lag. Analysis of North American Regional Reanalysis (NARR) between 1950 and 2010 reveals that upwelling, forced by alongshore winds, decreases in frequency and duration northward along the west coast of North America [*Bylhouwer et al.*, 2013]. Recent analysis of NARR data has

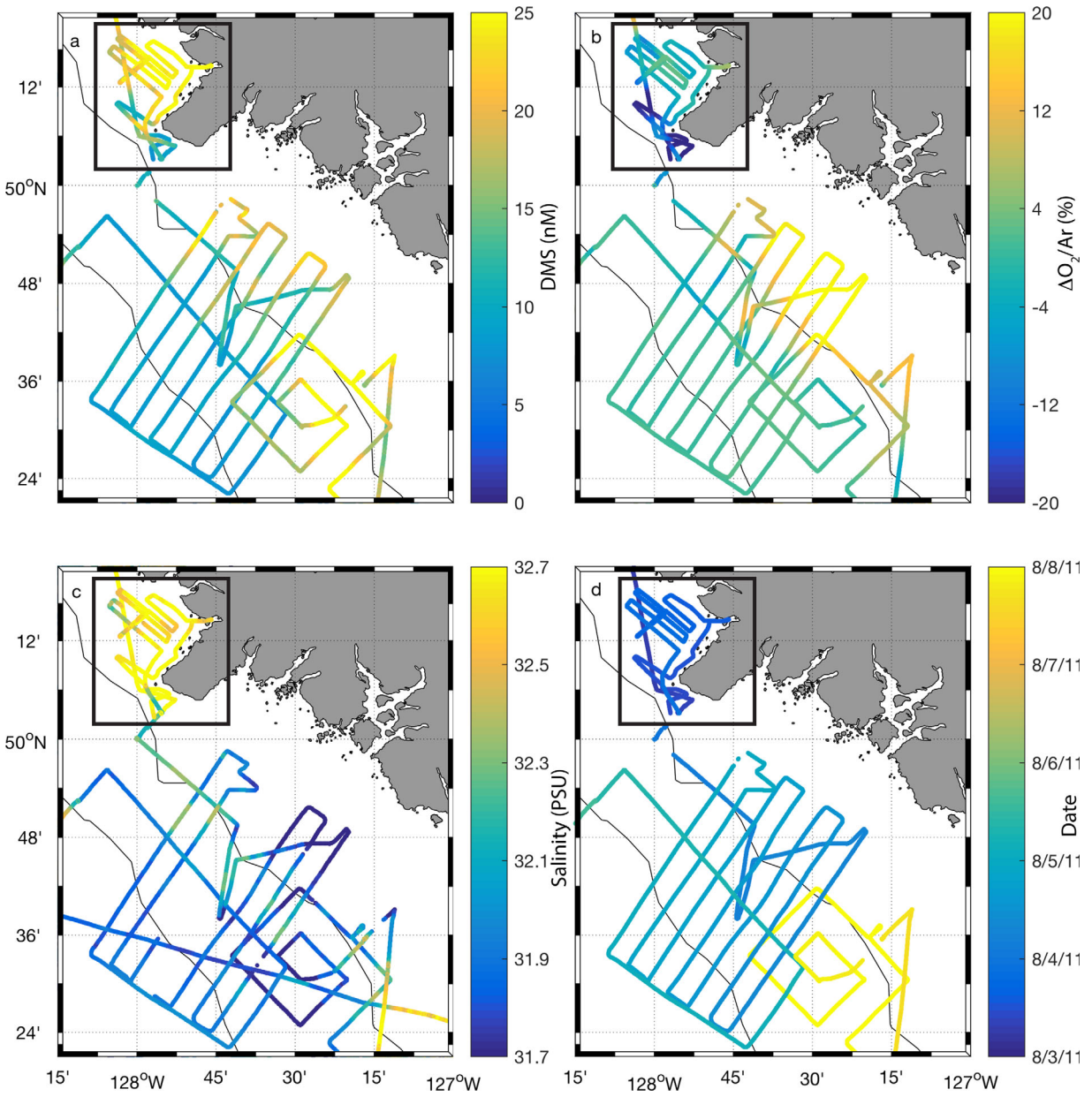

Figure 5. Detailed view of (a) DMS concentrations, (b) $\Delta O_2/Ar$, (c) salinity, and (d) sampling date in surface waters (~5 m) along the West Coast of Vancouver Island near the Brooks Peninsula in July 2010. The box denotes an upwelling plume as indicated by low temperature, high salinity waters.

revealed a coherence of the upwelling intensity between 36°N and 51°N and alongshore (upwelling) winds at 36°N at various time lags [*Engida et al.*, 2016]. The 36°N upwelling signal is visible in the uplift of deep isotherms and reaches Vancouver Island in approximately four days from off the coast of California.

Despite some regional coherence between DMS concentrations and surface salinity, there was no overall correlation between these variables across oceanographic regimes. Similarly, we did not find any statistically significant correlations between surface DMS concentrations Chl*a*, MLD (Figures 3a and 3b) or underway sea surface temperature (data not shown). We did, however, observe a weak correlation between DMS and the combined Haptophyte and Dinoflagellate Chl*a* (μg L^{-1}) across all stations (Figure 3c; $r^2 = 0.10$, $p < 0.05$) and between DMS and the CHL/MLD (mg m^{-2}) ratio binned to 1 × 1 degree as per the algorithm of *Simo and Dachs* [2002] ($r^2 = 0.31$, $p < 0.001$). The slope of the DMS versus CHL/MLD (mg m^{-2}) relationship we found for our data set (12.0 ± 1.0) was virtually identical to that reported previously by *Tortell et al.* [2012b] for the coastal Subarctic Pacific. In the original work of Simo and Dachs, CHL/MLD values greater than 1

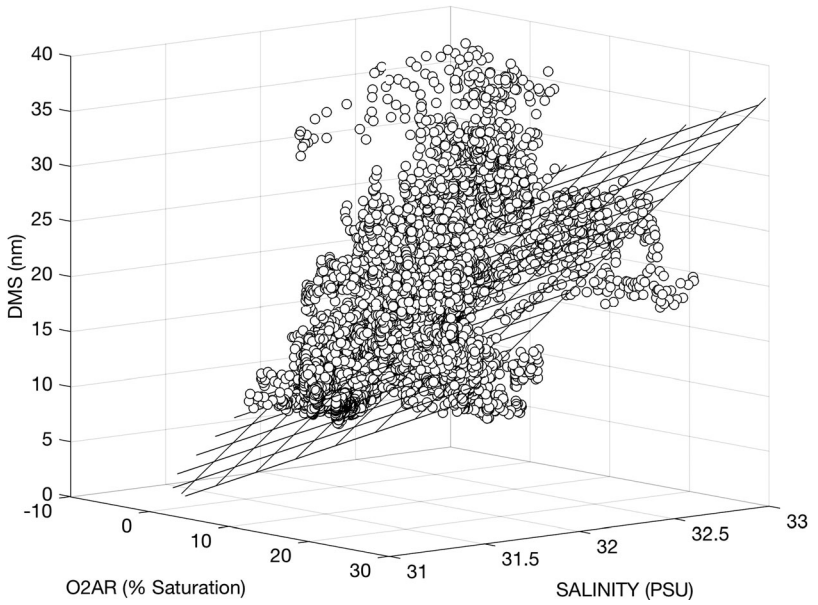

Figure 6. Multiple regression of DMS against salinity and $\Delta O_2/Ar$ in surface waters (~5 m) along the West Coast of Vancouver Island near the Brooks Peninsula in July 2010. The plane of best fit is shown in gray mesh (DMS = −462 + 0.38 $\Delta O_2/Ar$ + 14.8 Sal; $r^2 = 0.56$ F-stat = 7607, $p < 0.01$).

were excluded from the analysis. Indeed, we found that the apparent correlation broke down at CHL/MLD ratios > 0.8. We did not find a significant relationship between surface DMS concentrations and solar radiation dose [*Vallina and Simo*, 2007].

3.5. Discrete DMS/P/O Concentration Measurements

In addition to our MIMS-based continuous DMS observations, we also made discrete measurements of DMS, DMSP and DMSO along the Line P transect in 2011 (Table 2). Unfortunately, concentrations for DMSP and DMSO were not measured on the WCAC cruise in 2010. We measured $DMSP_t$ concentrations ranging from 22 to 96 nM, and DMS concentrations ranging from 0.46 to 33 nM. The discrete DMS concentrations were consistent with our continuous MIMS measurements, while our DMSPt measures are consistent with published values of particulate DMSP for the Subarctic Pacific [*Royer et al*., 2010; *Steiner et al*., 2012]. Our $DMSP_d$ measurements showed concentrations ranging from 1.3 to 8.3 nM, in good agreement with $DMSP_d$ measurements along Line P in 2011 (M. Robert, personal communication, 2014). Due to a bottle labeling problem, we were forced to average $DMSO_d$ samples from the coastal and transitional stations (P4-P12), which limits our ability to discern $DMSO_d$ variability among coastal/transitional waters. Nonetheless, the averaged $DMSO_d$ concentrations we measured (range 13.4-23 nM; Table 2) were higher than previous values obtained in the Subarctic Pacific [*Asher et al*., 2015; *Bates et al*., 1994], likely reflecting seasonal and inter-annual variability.

Table 2. Surface Water (~5 m) Concentrations of Reduced-Sulfur Compounds in Along Line P[a]

Station	Region	DMS (nM)	$DMSP_d$(nM)	$DMSP_t$(nM)	$DMSO_d$ (nM)
P2	Coastal	1.6 ± 1.3	2.4 ± 0.4	50 ± 1.1	23 ± 13
P4	Coastal	3.8 ± 1.2	1.4 ± 1.8	54 ± 6.1	23 ± 13
P9	Transitional	4.7 ± 2.2	2.1 ± 0.10	33 ± 2.8	23 ± 13
P12	Transitional	11 ± 1.8	8.3 ± 3.5	96 ± 4.7	23 ± 13
P16	Oceanic	3.5 ± 1.5	3.0 ± 0.14	51 ± 0.4	19.6 ± 3.0
P20	Oceanic	8.0 ± 1.1	1.3 ± 0.32	22 ± 1.7	13.4 ± 2.8
P26	Oceanic	12 ± 1.0	6.3 ± 3.5	31 ± 4.4	20.9 ± 5.8

[a]Mean concentrations ± one standard error measured at discrete sampling stations in August 2011. Due a labeling error, $DMSO_d$ samples from stations P2-P12 could not be distinguished from one another. These samples were thus pooled, and the values represent the mean and standard deviation of surface waters between P2 and P12. DMSP and DMSO measurements were made on duplicate samples, while DMS measurements were made on single samples.

Table 3. Mean Rates of Gross DMS Production, Gross DMS Removal, and Net DMS Production[a]

Station	Zone	Lat. (°N)	Long. (°E)	Gross DMS Cons. (d^{-1})	DMSP Cleav. (d^{-1})	DMSO Red. (d^{-1})	Net Production (d^{-1})
ML1	C	47.86	−125.05	−1.1 ± 1.4	-	-	−0.21 ± 0.40
BP3	C	50.05	−127.92	−1.1 ± 0.59	-	-	0.27 ± 0.25
QCS1	C	50.72	−128.67	−3.2± 2.2	-	-	−0.099 ± 0.22
QCS5	C	50.58	−129.00	−0.70 ± 0.47	-	-	−0.04 ± 0.09
HIS	C	52.63	−131.37	−1.6 ± 1.2	-	-	−0.10 ± 0.16
DE1	C	54.42	−132.30	−1.1± 2.9	-	-	−0.85 ± 0.48
DE6	T	53.81	−134.25	−0.48 ± 0.30	-	-	0.01± 0.25
DE9	T	53.11	−135.60	−0.72 ± 0.83	-	-	−0.72± 0.13
QCS9	T	50.10	−130.18	−0.33 ± 0.70	-	-	−0.42 ± 0.75
P4	C	48.65	−126.67	−1.1 ± 0.4	1.0 ± 0.72	0.11 ± 1.0	−0.50 ± 0.7
P9	T	48.89	−129.66	−1.9 ± 1.0	1.7 ± 1.4	n.d.	−1.1 ± 0.9
P12	T	48.97	−130.67	−1.3 ± 0.38	1.7± 0.14	0.25 ± 0.22	0.47 ± 0.20
P20	O	49.57	−138.67	−0.22 ± 0.03	1.3 ± 0.61	n.d.	−0.01 ± 0.7
P26	O	50.00	−145.00	−0.48 ± 0.2	1.2 ±0.60	n.d.	0.20 ± 0.7

[a]Measurements (mean ± one standard error) derived from DMS competitive inhibitor experiments on the WCAC cruise in 2010, and mean rates (± one standard error) of gross DMS removal, DMSP cleavage, DMSO reduction, and net DMS production at the major stations along the Line P transect in August, 2011. Rates below detection (i.e., no measurable changes in tracer concentrations) are listed as n.d. Missing data are indicated with a dash. C, T, and O represent stations determined to be in the coastal, transition and, oceanic zones, respectively.

3.6. Sea-Air Fluxes

We calculated DMS fluxes in open-ocean, transitional, and coastal waters, combining aqueous DMS data from our two cruises (Table 1). Maximum sea-air flux (100 um m^{-2} d^{-1}) was observed in the open ocean, with values decreasing toward the coastal region. As noted above, both coastal and open ocean waters contained high aqueous DMS concentrations, with the oceanic-coastal gradient sea-air flux driven by higher wind speeds in the open ocean (6.0 ± 2.6 m s^{-1}) and the transitional region (5.3 ± 2.3 m s^{-1}) relative to the coastal waters (3.9 ± 1.2 m s^{-1}). This result suggests that overall the waters of the Subarctic Northeast Pacific are a significant summer-time source of atmospheric DMS.

3.7. Rate Constants of DMS Production and Removal

In Table 3, we present rate constants of gross DMS production, gross DMS removal, and net DMS production derived from stable isotope CI at all of the sampling stations on the WCAC cruise. Rate constants of gross DMS removal, DMSP cleavage, DMSO reduction, and net DMS production along the Line P transect are also summarized in Table 3. Across our sampling stations, turnover times for DMS ranged between 0.5 and 4.5 days, and averaged 0.87 ± 0.34 days in coastal waters, 2.0 ± 1.4 days in transitional waters, and 3.5 ± 2.1 days in open ocean waters, respectively. Gross DMS production rate constants were generally lower than gross DMS removal rate constants, resulting in negative net DMS production and suggesting net removal of DMS from surface waters. Indeed, at three out of five stations, net DMS production was negative, indicating that DMS removal exceeded production. In all cases, the sum of the gross production and removal rate terms is consistent with the measured net production term, within the measurement errors. We observed considerable variability in rate constants of net DMS production (−0.17 ± 0.50 d^{-1}) gross DMS removal (mean −1.0 d^{-1} ± 0.68 d^{-1}), $DMSO_d$ reduction (0.12 ± 0.20 d^{-1}), and to a lesser extent, $DMSP_d$ cleavage (1.4 d^{-1} ± 0.31 d^{-1}). $DMSP_d$ cleavage was higher than DMSO reduction between P8 and P26, and the highest rates of $DMSP_d$ cleavage were observed in the offshore waters due to substantial $DMSP_d$ pools (see Table 2).

3.8. Patterns in DMS Production and Removal Terms

Rate constants for net DMS production across the full survey region in 2010 and 2011 were positively correlated with surface water DMS concentrations, as shown in Figure 7a ($r^2 = 0.62$, $p < 0.05$, n = 14; Figure 7). Limited data prevent the identification of any strong spatial patterns in net DMS production (Figure 7b) or gross DMS removal (data not shown). However, we did find a statistically significant positive correlation between gross DMS production constants in coastal and transitional waters with the upwelling index ($r^2 = 0.50$, $p < 0.05$, n = 9). Gross DMS production and net DMS production were not correlated with Haptophyte and Dinoflagellate Chl*a* concentrations or other hydrographic variables.

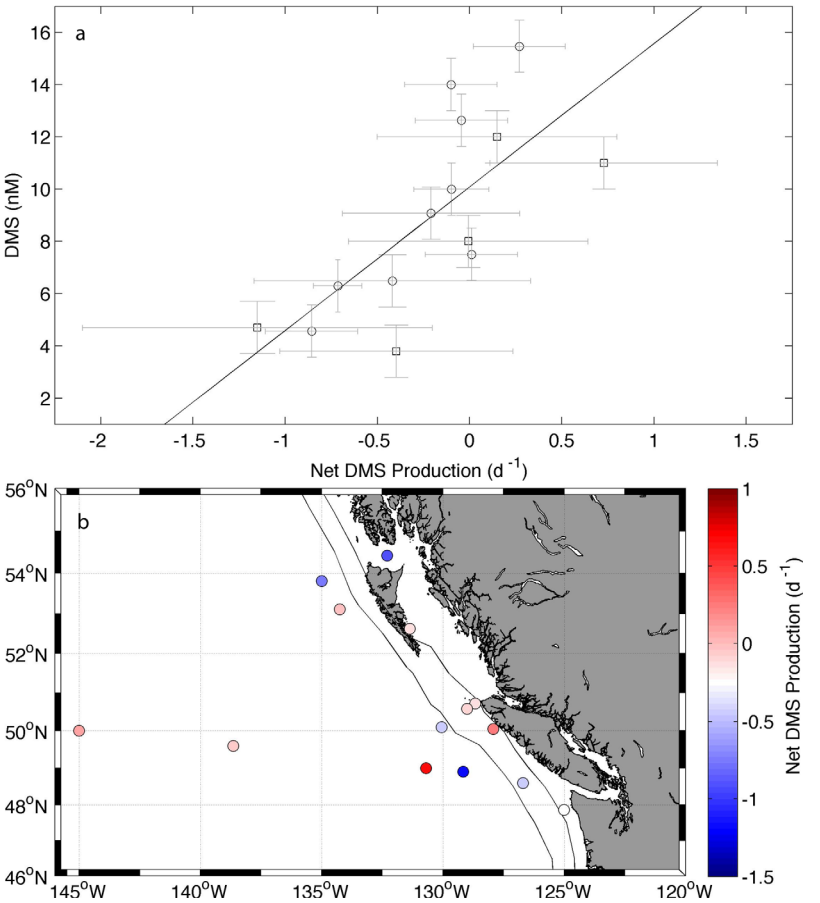

Figure 7. (a) Relationship between measured rate constants of net DMS production (d^{-1}) and surface water DMS concentrations in the Subarctic NE Pacific. The line represents the best-fit linear regression ($r^2 = 0.62$, $p < 0.05$, n = 14; DMS = 5.49 × net DMS prod + 10.1, and (b) the spatial distribution of net DMS production rate constants (d^{-1}) in coastal and offshore waters of the Subarctic Pacific during 2010 and 2011. The 500 m and 2000 m isobaths are included for reference.

4. Discussion

The results presented here constitute the most complete regional survey of DMS/P/O concentrations and production/removal rates in surface waters of the Subarctic NE Pacific. This study corroborates the few existing data on gross DMS removal, and provides the first measurements of DMS removal and turnover in continental shelf waters, and the first direct comparison of DMSP cleavage and DMSO reduction as sources of DMS in the Subarctic Pacific (Figure 1). Below, we discuss our results in terms of currently existing data, and show how our new observations extend existing knowledge of DMS dynamics in this region.

4.1. Strong Spatial Gradients in DMS Concentrations and Sea-Air Fluxes

Using automated MIMS analysis of surface waters, we were able to map the distribution of DMS concentrations in coastal and open ocean waters of the Subarctic Pacific with high spatial resolution. DMS concentrations appeared higher and more heterogeneous in coastal and open ocean waters than in transitional waters (Figure 4 and Table 1). DMS measurements obtained near the Brooks Peninsula (Figure 5) exemplified the strong spatial variability we observed in near-shore coastal waters. A multilinear regression of the high-resolution data collected in this region revealed that $\Delta O_2/Ar$ and salinity could explain a sizable fraction of the variance in DMS concentrations (~0 – 40 nM). This result suggests that recently upwelled, saline waters and phytoplankton productivity (driving the supersaturation of ΔO2/Ar) provided favorable conditions for DMS accumulation. In the absence of N_2O measurements, $\Delta O_2/Ar$ ratios were not corrected for vertical mixing (i.e., upwelling, entrainment, or dypicnal mixing) using the recent method of *Cassar et al.* [2014]. As a result, our $\Delta O_2/Ar$ measurements reflect an in situ signature of net community production and the potential influence of mixing dynamics that bring O_2 under-saturated waters into the mixed layer.

ΔO_2/Ar measurements thus represent a likely under-estimate of the true biological productivity signal. On short timescales (~3 days), we might expect a stronger correlation between ΔO_2/Ar and DMS, if the ΔO_2/Ar measurements had been corrected for vertical mixing. However, the integration timescales of ΔO_2/Ar is ~7 to 14 days, whereas DMS turnover in the surface ocean occurs on much shorter timescales (1–4 days). Thus, we hypothesize that the uncoupling between ΔO_2/Ar and DMS occurs when biological DMS consumption (nM d^{-1}) outpaces the heterotrophic removal of oxygen (μmol d^{-1}).

Overall, data from the 2010 WCAC cruise agree well with the observations of *Tortell et al*. [2012b] and *Nemek et al*. [2008], who documented high DMS concentrations and spatial variability along the West Coast of Vancouver Island and in the Queen Charlotte Sound. Our results thus provide further evidence that this is a region of persistently high summer time DMS concentrations. During the 2011 Line P cruise, we observed less variability in coastal DMS concentrations. This may reflect the less extensive sampling of coastal and transitional waters during this cruise relative to the WCAC survey in 2010. The dominant spatial gradient along the Line P cruise track was associated with the transition from iron-replete to iron-limited waters west of ~137° (as judged from surface NO_3^- data). In addition, a small-scale DMS "hotspot" was observed at ~130.7°W, corresponding with a hydrographic front, as indicated by a strong surface salinity gradient. This region has previously been identified as a biological productivity hotspot [*Ribalet et al*., 2010], influenced by the mixing of high Fe coastal waters, with high NO_3^- offshore waters. Our results from the 2011 Line P cruise are consistent with the observations of *Steiner et al*. [2012], who documented persistently high summer (August) DMS concentrations in open-ocean waters between 1996 and 2010. Combined with high offshore winds, these persistently elevated oceanic DMS concentrations result in large sea-air DMS fluxes that agree well with the range of the long-term climatological means derived by *Lana et al*. [2011] for the Subarctic NE Pacific. Our results thus support previous observations showing that this region represents an important summer time source of atmospheric sulfur.

4.2. DMSP/O Concentrations in the Subarctic NE Pacific

As in previous studies [*Levasseur et al*., 2006; *Royer et al*., 2010], we found that concentrations of total and particulate DMSP were similar. The result reflects the dominance of the $DMSP_p$ pool compared to the $DMSP_d$ pool. Apparent differences in $DMSP_d$ concentrations between datasets [e.g., this one and *Royer et al*., 2010] highlight strong interannual and seasonal variability, as well as spatial variability among sampling sites in the various subregions. Artifacts related to sample handling could also lead to an additional source of variability in measured $DMSP_d$ concentrations. Phytoplankton cell lysis during filtration has been shown to release substantial amounts of particulate DMSP into the dissolved pool, leading to artificially high $DMSP_d$ concentrations. While we cannot rule out potential sampling artifacts, we and other authors working along Line P have followed the protocol recommended by *Kiene and Slezak* [2006] to minimize cell disruption during the filtration process.

Only two previous studies have reported DMSO concentrations in the Subarctic Pacific. *Bates et al*. [1994] measured $DMSO_t$ from 5 to 60 m at the PSI-3 time series station in southern coastal waters (~128°W 48°N) in April, which is prior to the onset of the upwelling season. Their results showed maximum DMSO concentrations of 5 nM. By comparison, $DMSO_d$ values in all of the regions we sampled (i.e., coastal, transitional, and open-ocean waters) were substantially higher than this (range 13–23, mean 20.4 nM). The higher concentrations we observed relative to *Bates et al*. [1994] likely reflect the difference in sampling time (late-summer vs. early spring), and the role of DMS photo-oxidation in the formation of $DMSO_d$ [*Toole et al*., 2003; *Bouillon et al*., 2006]. Our own recent measurements [*Asher et al*., 2015] demonstrate high $DMSO_{d/t}$ concentrations along Line P during August of 2014, with a mean value of ~11 nM. These additional data suggest persistently high summer-time DMSO concentrations in the NE Subarctic Pacific. As discussed below, the role of the DMSO pool in DMS dynamics requires further study.

4.3. Trends in DMS Production/Removal

We observed a positive correlation between surface water DMS concentrations and the rates of net DMS production across our study area (Figure 7). This correlation suggests that our rate measurements capture the majority of processes driving DMS accumulation in the Subarctic NE Pacific (we note that macrozooplankton grazing, vertical mixing, horizontal advection, which may be important on short timescales, are not well represented). Higher rates could be related to higher rates of bacterial metabolism in coastal waters, driven by greater phytoplankton biomass (chl*a*) and productivity (biological O_2 supersaturation,

ΔO_2/Ar; Figure 3b). Across our study area, DMS turnover times ranged between < 1day and ~4 days, which is consistent with previous studies [e.g., *Merzouk et al*., 2006]. Shorter turnover times in coastal waters (< 1 day) are sufficient to remove any signature of DMS accumulation, thus effectively "resetting" the mixed layer DMS budget on short time scales. Rapid DMS turnover in coastal waters also explains the greater spatial variability we observed in DMS concentrations.

Our measured gross DMS removal and production rates represent a combination of biological and abiotic (e.g., photo-oxidation) processes, but they do not take into account physical processes such as mixing and sea-air exchange (e.g., Figure 1). Calculations of sea-air flux demonstrate that this is generally a minor term in the DMS budget of the Subarctic Pacific, with maximum removal of DMS averaging 0.64 ± 0.68 nM d^{-1} and equivalent rate constants of 0.10 ± 0.084 d^{-1}. The rate constants associated with sea-air flux thus represent an average of ~8% of the total DMS removal we measured in the surface layer. There were, however, two instances (station DE9 and P20) where sea-air flux accounted for between 30 and 50% of measured gross DMS removal rates. We estimated maximum DMS photo-oxidation rate constants by scaling published values from *Bouillon et al*. [2006] from the Subarctic Northeast Pacific by in situ nitrate concentrations and short wave radiation measurements, obtained from http://www.pmel.noaa.gov/OCS/data/disdel_v2/disdel_v2.html. *Bouillon et al*. [2006] showed that the DMS quantum yield is well correlated with nitrate concentrations (DMS = 0.15 NO_3 + 0.41), and *Bouillon et al*. [2006] demonstrated that changes in nitrate concentrations and solar radiation resulted in the largest changes in DMS photo-oxidation rate constants (± ~50%) in surface waters. Our estimates of DMS photo-oxidation ranged between ~0.027 and 0.15 d^{-1}. On average, these values represent ~20% of gross DMS removal across our study area, though at some high NO_3^- stations (e.g., P20), photo-oxidation can account as much as ~70% of measured gross DMS removal. To estimate the potential for mixing at the base of the mixed layer to dilute DMS concentrations in surface waters (Figure 1), we used simple box model calculations based on the work of *Ianson and Allen* [2002] derived specifically for coastal BC waters. This calculation indicated that DMS removal due to mixing at the base of the mixed layer was also small (≤0.03 nMd^{-1}). Thus, our results indicate that biological processes generally dominated DMS removal compared to sea-air flux, photo-oxidation, and mixing at the base of the mixed layer (see Figure 1). *Yang et al*. [2013] reached a similar conclusion regarding the dominance of biological consumption on the removal of DMS during So GasEx in the Southwest Atlantic sector of the Southern Ocean, which is also an oceanographic region characterized by high DMS concentrations and heterogeneity.

Given the strong density stratification of surface waters across the offshore Subarctic Pacific (due to a low salinity surface layer), vertical entrainment of subsurface waters is not likely a strong DMS sink (or source). In coastal waters, however, upwelling could potentially decrease mixed layer DMS concentrations (Figure 1), given the low DMS concentrations in subsurface waters [*Wong et al*., 2005; *Steiner et al*., 2012]. Our detailed 2010 survey of the Brooks Peninsula (Figure 5) showed that DMS accumulation began within one day of upwelling, with high DMS water masses subsequently advected offshore, and DMS concentrations attenuated, likely by rapid biological consumption. The short turnover of DMS (< 1 day) at station BP3 following the SAR transects survey, and a similarly short average turnover in coastal surface waters, suggests that DMS accumulation can be attenuated over short temporal and spatial scales. These high rate constants of DMS turnover can help to explain the significant temporal variability we observed in the Brooks Peninsula SAR region (Figure 5).

4.4. A Comparison of Available Rate Measurements From the Subarctic NE Pacific

To date, three different methods have been used to examine DMS cycling in the NE Subarctic Pacific; competitive inhibition assays, stable isotope tracer additions and radio isotopes [e.g., *Royer et al*., 2010; *Merzouk et al*., 2006]. The available data show good agreement (within 0.05 d^{-1}) in terms of DMS consumption rates at Station P26, despite differences in sampling years and methodology (Table 3), providing confidence in the available measurements. DMSP cleavage rates at Line P stations agree within a factor of 2–4. Measurements of DMSP cleavage rates in spring (May/June) along Line P have produced estimates averaging ~0.5 ± 0.3 d^{-1}, with values ranging from 0.14 to ~0.83 d^{-1} [*Royer et al*., 2010]. By comparison, we measured an average $DMSP_d$ cleavage rate of ~1.4 ± 0.4 d^{-1} (Table 3). We expect higher rates of $DMSP_d$ cleavage in summer than spring, to sustain the elevated open-ocean DMS concentrations frequently observed in August in the Subarctic Northeast Pacific.

Our results provide the first $DMSO_d$ reduction rate constants in the Subarctic Pacific. We found that rate constants of $DMSO_d$ reduction were significantly lower than $DMSP_d$ cleavage and gross DMS removal except in coastal waters (Table 3). However, since $DMSO_d$ pool sizes are often comparable or larger than $DMSP_d$ pool sizes (Table 2), $DMSO_d$ reduction can provide an important source of DMS in the Subarctic NE Pacific. Additional DMSO concentration and reduction rate measurements are thus needed (both in coastal and open ocean waters) to better characterize the importance of this compound in the DMS cycle of the Subarctic Pacific. As both an important sink of DMS through photo-oxidation and biological oxidation, and as a source of DMS from DMSO reduction, DMSO measurements should be included in future DMS research programs. We have recently developed an automated method for surface DMSO (and DMS/P) measurements [*Asher et al*., 2015], which will enable future research into the spatial distribution of this compound in marine surface waters.

5. Conclusions and Future Outlook

This study provides extensive coverage of DMS/P/O concentrations and cycling in open-ocean and coastal regions of the Subarctic NE Pacific. We observed high DMS concentrations and sea-air fluxes across the region, further demonstrating the importance of the Subarctic NE Pacific as an important source of DMS to the atmosphere. DMS concentrations in surface waters were correlated with standard oceanographic variables on various temporal and spatial scales, although these empirical relationships did not have significant predictive power. In contrast, we found that measured net DMS production rates were strongly correlated to surface water DMS concentrations across our survey region. Our results show that rates of DMS production and removal vary across and within oceanographic regimes, and this variability, driven by a range of oceanographic factors, can explain the dominant gradients in surface water DMS accumulation. The rapid DMS turnover times reported in coastal waters help explain the presence of localized DMS "hotspots," as compared to the more homogeneous DMS accumulation in the HNLC open-ocean.

Further studies are needed to examine the physical and biological drivers of production and removal terms in the Subarctic Pacific DMS cycle, and to document the seasonality of DMS dynamics across the contrasting coastal and offshore oceanographic regimes. Additional measurements are needed to better parameterize and validate regional biogeochemical models [e.g. *Steiner and Denman*, 2008] examining the response of Subarctic NE Pacific surface waters along Line P to on-going climate-dependent perturbations.

Acknowledgments
We would like to thank the Line P chief scientist Marie Robert, colleagues Dave Semeniuk, Ania Posacka, and Nina Schuback from the University of British Columbia for their help with sampling, and the Institute of Ocean Sciences-Fisheries and Oceans Canada for providing ancillary data. For access to the data used, please email ecasher@ucdavis.edu. Funding for this work was provided by a Discovery Grant from the Natural Sciences and Engineering Research Council of Canada, from the Peter Wall Institute for Advanced Studies.

References

Asher, E. C., A. Merzouk, and P. D. Tortell (2011a), Fine-scale spatial and temporal variability of surface water dimethylsufide (DMS) concentrations and sea–air fluxes in the NE Subarctic Pacific, *Mar. Chem.*, *126*(1-4), 63–75, doi:10.1016/j.marchem.2011.03.009.

Asher, E. C., J. W. H. Dacey, M. M. Mills, K. R. Arrigo, and P. D. Tortell (2011b), High concentrations and turnover rates of DMS, DMSP and DMSO in Antarctic sea ice: DMS dynamics in Antarcic sea ice, *Geophys. Res. Lett.*, *38*, L23609, doi:10.1029/2011GL049712.

Asher, E. C., J. W. H. Dacey, T. Jarniková, and P. D. Tortell (2015), Measurement of DMS, DMSO, and DMSP in natural waters by automated sequential chemical analysis: Sequential measurement of DMS, DMSO, and DMSP, *Limnol. Oceanogr. Methods*, *13*(9), 451–462, doi:10.1002/lom3.10039.

Barwell-Clarke, J., and F. Brabant (1996), Institute of Ocean Sciences nutrient methods and analysis, *Can. Tech. Rep. Hydrogr. Ocean Sci.*, *182*, vi+43.

Bates, T. S., R. P. Kiene, G. V. Wolfe, P. A. Matrai, F. P. Chavez, K. R. Buck, B. W. Blomquist, and R. L. Cuhel (1994), The cycling of sulfur in surface seawater of the northeast Pacific, *J. Geophys. Res.*, *99*(C4), 7835–7843, doi:10.1029/93JC02782.

Belviso, S., L. Bopp, C. Moulin, J. C. Orr, T. R. Anderson, O. Aumont, S. Chu, S. Elliott, M. E. Maltrud, and R. Simo (2004), Comparison of global climatological maps of sea surface dimethyl sulfide, *Global Biogeochem. Cycles*, *18*, GB3013, doi:10.1029/2003gb002193.

Bouillon, R. C., and W. L. Miller (2005), Photodegradation of dimethyl sulfide (DMS) in natural waters: Laboratory assessment of the nitrate-photolysis-induced DMS oxidation, *Environ. Sci. Technol.*, *39*(24), 9471–9477, doi:10.1021/es048022z.

Bouillon, R. C., W. L. Miller, M. Levasseur, M. Scarratt, A. Merzouk, S. Michaud, and L. Ziolkowski (2006), The effect of mesoscale iron enrichment on the marine photochemistry of dimethylsulfide in the NE subarctic Pacific, *Deep Sea Res., Part II*, *53*(20-22), 2384–2397, doi:10.1016/j.dsr2.2006.05.024.

Brainerd, K. E., and M. C. Gregg (1995), Surface mixed and mixing layer depths, *Deep Sea Res., Part I*, *42*(9), 1521–1543, doi:10.1016/0967-0637(95)00068-h.

Bylhouwer, B., D. Ianson, and K. Kohfeld (2013), Changes in the onset and intensity of wind-driven upwelling and downwelling along the North American Pacific coast: Upwelling and downwelling in North CCS, *J. Geophys. Res. Oceans*, *118*, 2565–2580, doi:10.1002/jgrc.20194.

Cassar, N., C. D. Nevison, and M. Manizza (2014), Correcting oceanic O_2/Ar-net community production estimates for vertical mixing using N_2O observations: Composite N_2O-O_2/Ar tracer of NCP, *Geophys. Res. Lett.*, *41*, 8961–8970, doi:10.1002/2014GL062040.

Charlson, R. J., J. E. Lovelock, M. O. Andreae, and S. G. Warren (1987), Oceanic phytoplankton, atmospheric sulfur, cloud albedo and climate, *Nature*, *326*(6114), 655–661.

Cullen, J. T., M. Chong, and D. Ianson (2009), British Columbian continental shelf as a source of dissolved iron to the subarctic northeast Pacific Ocean, *Global Biogeochem. Cycles*, *23*, GB4012, doi:10.1029/2008GB003326.
Dacey, J. W. H., F. A. Howse, A. F. Michaels, and S. G. Wakeham (1998), Temporal variability of dimethylsulfide and dimethylsulfoniopropionate in the Sargasso Sea, *Deep Sea Res., Part I*, *45*(12), 2085–2104, doi:10.1016/S0967-0637(98)00048-X.
Ditullio, G. R., and W. O. Smith (1995), Relationship between dimethylsulfide and phytoplankton pigment concentrations in the Ross Sea, Antarctica, *Deep Sea Res., Part I*, *42*(6), 873–892, doi:10.1016/0967-0637(95)00051-7.
Engida, Z., A. Monahan, D. Ianson, and R. E. Thomson (2016), Remote forcing of subsurface currents and temperatures near the northern limit of the California current system, *J. Geophys. Res. Oceans*, *121*, 7244–7262, doi:10.1002/2016JC011880.
Evans, W., B. Hales, P. G. Strutton, and D. Ianson (2012), Sea-air CO2 fluxes in the western Canadian coastal ocean, *Prog. Oceanogr.*, *101*(1), 78–91, doi:10.1016/j.pocean.2012.01.003.
Freeland, H. J., W. R. Crawford, and R. E. Thomson (1984), Currents along the pacific coast of Canada, *Atmos. Ocean*, *22*(2), 151–172, doi:10.1080/07055900.1984.9649191.
Halloran, P. R., T. G. Bell, and I. J. Totterdell (2010), Can we trust empirical marine DMS parameterisations within projections of future climate?, *Biogeosciences*, *7*(5), 1645–1656, doi:10.5194/bg-7-1645-2010.
Harrison, P. J., P. W. Boyd, D. E. Varela, and S. Takeda (1999), Comparison of factors controlling phytoplankton productivity in the NE and NW subarctic Pacific gyres, *Prog. Oceanogr.*, *43*(2-4), 205–234, doi:10.1016/S0079-6611(99)00015-4.
Ho, D. T., C. S. Law, M. J. Smith, P. Schlosser, M. Harvey, and P. Hill (2006), Measurements of air-sea gas exchange at high wind speeds in the Southern Ocean: Implications for global parameterizations, *Geophys. Res. Lett.*, *33*, L20604, doi:10.1029/2006GL028295.
Holm-Hansen, O., C. J. Lorenzen, R. W. Holmes, and J. D. H. Strickland (1965), Fluorometric determination of chlorophyll, *ICES J. Mar. Sci.*, *30*(1), 3–15, doi:10.1093/icesjms/30.1.3.
Howard, E. C., et al. (2006), Bacterial taxa that limit sulfur flux from the ocean, *Science*, *314*(5799), 649–652, doi:10.1126/science.1130657.
Ianson, D., and S. E. Allen (2002), A two-dimensional nitrogen and carbon flux model in a coastal upwelling region: Coastal nitrogen and carbon flux model, *Global Biogeochem. Cycles*, *16*(1), 1011, doi:10.1029/2001GB001451.
Kiene, R. P., and D. Slezak (2006), Low dissolved DMSP concentrations in seawater revealed by small-volume gravity filtration and dialysis sampling, *Limnol. Oceanogr. Methods*, *4*, 80–95, doi:10.4319/lom.2006.4.80.
Kiene, R. P., L. J. Linn, and J. A. Bruton (2000), New and important roles for DMSP in marine microbial communities, *J. Sea Res.*, *43*(3-4), 209–224, doi:10.1016/s1385-1101(00)00023-x.
Lana, A., et al. (2011), An updated climatology of surface dimethlysulfide concentrations and emission fluxes in the global ocean, *Global Biogeochem. Cycles*, *25*, GB1004, doi:10.1029/2010GB003850.
Le Clainche, Y., et al. (2006), Modeling analysis of the effect of iron enrichment on dimethyl sulfide dynamics in the NE Pacific (SERIES experiment), *J. Geophys. Res. Oceans*, *111*, C01011, doi:10.1029/2005JC002947.
Le Clainche, Y., et al. (2010), A first appraisal of prognostic ocean DMS models and prospects for their use in climate models, *Global Biogeochem. Cycles*, *24*, GB3021, doi:10.1029/2009GB003721.
Levasseur, M., et al. (2006), DMSP and DMS dynamics during a mesoscale iron fertilization experiment in the Northeast Pacific - Part I: Temporal and vertical distributions, *Deep Sea Res., Part II*, *53*(20-22), 2353–2369, doi:10.1016/j.dsr2.2006.05.023.
Levine, N. M., V. A. Varaljay, D. A. Toole, J. W. H. Dacey, S. C. Doney, and M. A. Moran (2012), Environmental, biochemical and genetic drivers of DMSP degradation and DMS production in the Sargasso Sea, *Environ. Microbiol.*, *14*(5), 1210–1223, doi:10.1111/j.1462-2920.2012.02700.x.
Levitus, S. (1982), Climatological atlas of the world ocean, NOAA Prof. Pap. 13, 173 pp., U.S. Govt. Printing Off., Washington, D. C.
Lizotte, M., M. Levasseur, I. Kudo, K. Suzuki, A. Tsuda, R. P. Kiene, and M. G. Scarratt (2009), Iron-induced alterations of bacterial DMSP metabolism in the western subarctic Pacific during SEEDS-II, *Deep Sea Res., Part II*, *56*(26), 2889–2898, doi:10.1016/j.dsr2.2009.06.012.
Lovelock, J. E., R. J. Maggs, and R. A. Rasmussen (1972), Atmospheric dimethyl sulphide and the natural sulphur cycle, *Nature*, *237*(5356), 452–453, doi:10.1038/237452a0.
Mackey, M., D. Mackey, H. Higgins, and S. Wright (1996), CHEMTAX - a program for estimating class abundances from chemical markers: Application to HPLC measurements of phytoplankton, *Mar. Ecol. Prog. Ser.*, *144*, 265–283, doi:10.3354/meps144265.
Martin, J. H., and S. E. Fitzwater (1988), Iron-deficiency limits phytoplankton growth in the Northeast Pacific Subarctic, *Nature*, *331*(6154), 341–343, doi:10.1038/331341a0.
Masotti, I., et al. (2010), Spatial and temporal variability of the dimethylsulfide to chlorophyll ratio in the surface ocean: An assessment based on phytoplankton group dominance determined from space, *Biogeosciences*, *7*(10), 3215–3237, doi:10.5194/bg-7-3215-2010.
Merzouk, A., M. Levasseur, M. G. Scarratt, S. Michaud, R. B. Rivkin, M. S. Hale, R. P. Kiene, N. M. Price, and W. K. W. Li (2006), DMSP and DMS dynamics during a mesoscale iron fertilization experiment in the Northeast Pacific - Part II: Biological cycling, *Deep Sea Res., Part II*, *53*(20-22), 2370–2383, doi:10.1016/j.dsr2.2006.05.022.
Nemcek, N., D. Ianson, and P. D. Tortell (2008), A high-resolution survey of DMS, CO_2, and O_2/Ar distributions in productive coastal waters, *Global Biogeochem. Cycles*, *22*, GB2009, doi:10.1029/2006GB002879.
Nevitt, G. A. (2008), Sensory ecology on the high seas: The odor world of the procellariiform seabirds, *J. Exp. Biol.*, *211*(11), 1706–1713, doi:10.1242/jeb.015412.
Quinn, P. K., and T. S. Bates (2011), The case against climate regulation via oceanic phytoplankton sulphur emissions, *Nature*, *480*(7375), 51–56, doi:10.1038/nature10580.
Reisch, C. R., M. J. Stoudemayer, V. A. Varaljay, I. J. Amster, M. A. Moran, and W. B. Whitman (2011), Novel pathway for assimilation of dimethylsulphoniopropionate widespread in marine bacteria, *Nature*, *473*(7346), 208–211, doi:10.1038/nature10078.
Ribalet, F., A. Marchetti, K. A. Hubbard, K. Brown, C. A. Durkin, R. Morales, M. Robert, J. E. Swalwell, P. D. Tortell, and E. V. Armbrust (2010), Unveiling a phytoplankton hotspot at a narrow boundary between coastal and offshore waters, *Proc. Natl. Acad. Sci. U. S. A.*, *107*(38), 16,571–16,576, doi:10.1073/pnas.1005638107.
Royer, S. J., et al. (2010), Microbial dimethylsulfoniopropionate (DMSP) dynamics along a natural iron gradient in the northeast subarctic Pacific, *Limnol. Oceanogr.*, *55*(4), 1614–1626, doi:10.4319/lo.2010.55.4.1614.
Royer, S.-J., M. Galí, A. S. Mahajan, O. N. Ross, G. L. Pérez, E. S. Saltzman, and R. Simó (2016), A high-resolution time-depth view of dimethylsulphide cycling in the surface sea, *Sci. Rep.*, *6*, 32325, doi:10.1038/srep32325.
Saltzman, E. S., D. B. King, K. Holmen, and C. Leck (1993), Experimental-determination of the diffusion-coefficient of dimethylsulfide in water, *J. Geophys. Res.*, *98*(C9), 16,481–16,486.
Seymour, J. R., R. Simo, T. Ahmed, and R. Stocker (2010), Chemoattraction to dimethylsulfoniopropionate throughout the marine microbial food web, *Science*, *329*(5989), 342–345, doi:10.1126/science.1188418.

Sharma, S., L. A. Barrie, D. Plummer, J. C. McConnell, P. C. Brickell, M. Levasseur, M. Gosselin, and T. S. Bates (1999), Flux estimation of oceanic dimethyl sulfide around North America, *J. Geophys. Res.*, *104*(D17), 21,327–21,342, doi:10.1029/1999JD900207.

Simo, R., and J. Dachs (2002), Global ocean emission of dimethylsulfide predicted from biogeophysical data, *Global Biogeochem. Cycles*, *16*(4), 1078, doi:10.1029/2001GB001829.

Stefels, J., and L. Dijkhuizen (1996), Characteristics of DMSP-lyase in Phaeocystis sp (Prymnesiophyceae), *Mar. Ecol. Prog. Ser.*, *131*(1-3), 307–313, doi:10.3354/meps131307.

Steiner, N., and K. Denman (2008), Parameter sensitivities in a 1-D model for DMS and sulphur cycling in the upper ocean, *Deep Sea Res., Part I*, *55*(7), 847–865, doi:10.1016/j.dsr.2008.02.010.

Steiner, N. S., M. Robert, M. Arychuk, M. L. Levasseur, A. Merzouk, M. A. Peña, W. A. Richardson, and P. D. Tortell (2012), Evaluating DMS measurements and model results in the Northeast subarctic Pacific from 1996–2010, *Biogeochemistry*, *110*(1-3), 269–285, doi:10.1007/s10533-011-9669-9.

Sunda, W., D. J. Kieber, R. P. Kiene, and S. Huntsman (2002), An antioxidant function for DMSP and DMS in marine algae, *Nature*, *418*(6895), 317–320.

Toole, D. A., D. J. Kieber, R. P. Kiene, D. A. Siegel, and N. B. Nelson (2003), Photolysis and the dimethylsulfide (DMS) summer paradox in the Sargasso Sea, *Limnol. Oceanogr.*, *48*(3), 1088–1100, doi:10.4319/lo.2003.48.3.1088.

Tortell, P. D. (2005), Dissolved gas measurements in oceanic waters made by membrane inlet mass spectrometry, *Limnol. Oceanogr. Methods*, *3*, 24–37, doi:10.4319/lom.2005.3.24.

Tortell, P. D., C. Gueguen, M. C. Long, C. D. Payne, P. Lee, and G. R. DiTullio (2011), Spatial variability and temporal dynamics of surface water $pCO_{(2)}$, Delta O_2/Ar and dimethylsulfide in the Ross Sea, Antarctica, *Deep Sea Res., Part I*, *58*(3), 241–259, doi:10.1016/j.dsr.2010.12.006.

Tortell, P. D., M. C. Long, C. D. Payne, A.-C. Alderkamp, P. Dutrieux, and K. R. Arrigo (2012a), Spatial distribution of pCO_2, ΔO_2/Ar and dimethylsulfide (DMS) in polynya waters and the sea ice zone of the Amundsen Sea, Antarctica, *Deep Sea Res., Part II*, *71-76*, 77–93, doi:10.1016/j.dsr2.2012.03.010.

Tortell, P. D., A. Merzouk, D. Ianson, R. Pawlowicz, and D. R. Yelland (2012b), Influence of regional climate forcing on surface water pCO_2, ΔO_2/Ar and dimethylsulfide (DMS) along the southern British Columbia coast, *Cont. Shelf Res.*, *47*, 119–132, doi:10.1016/j.csr.2012.07.007.

Vallina, S. M., and R. Simo (2007), Strong relationship between DMS and the solar radiation dose over the global surface ocean, *Science*, *315*(5811), 506–508, doi:10.1126/science.1133680.

Wong, C. S., S. E. Wong, W. A. Richardson, G. E. Smith, M. D. Arychuk, and J. S. Page (2005), Temporal and spatial distribution of dimethylsulfide in the subarctic northeast Pacific Ocean: A high-nutrient-low-chlorophyll region, *Tellus, Ser. B*, *57*(4), 317–331.

Yang, M., S. D. Archer, B. W. Blomquist, D. T. Ho, V. P. Lance, and R. J. Torres (2013), Lagrangian evolution of DMS during the Southern Ocean gas exchange experiment: The effects of vertical mixing and biological community shift, *J. Geophys. Res. Oceans*, *118*, 6774–6790, doi:10.1002/2013JC009329.

Zapata, M., F. Rodriguez, and J. L. Garrido (2000), Separation of chlorophylls and carotenoids from marine phytoplankton: A new HPLC method using a reversed phase C-8 column and pyridine-containing mobile phases, *Mar. Ecol. Prog. Ser.*, *195*, 29–45, doi:10.3354/meps195029.